EVOLUTIONARY CONVERGENCE OF A NEURAL MECHANISM IN THE CAVEFISH LATERAL LINE SYSTEM

Sensory afferents are more active in blind cavefish

Elias T. Lunsford[1]*, Alexandra Paz*[2]*, Alex C. Keene*[2,3]*, and James C. Liao*[1]

[1]*The Whitney Laboratory for Marine Bioscience*

Department of Biology

University of Florida

Saint Augustine, FL USA 32080

[2]*Department of Biological Sciences*

Florida Atlantic University

Jupiter, FL USA 33458

[3]*Department of Biology*

Texas A&M University

College Station, TX USA 77843

Phone: 904-201-8404

Email: jliao@whitney.ufl.edu

Keywords: efference copy, corollary discharge, spontaneous activity, locomotion, hair cells

Number of pages: 27

Number of figures: 4

Numbers of words for abstract: 163/200

Numbers of words for introduction: 761

Number of words for discussion: 906

Conflict of Interest: The authors declare no competing financial interests.

Acknowledgements: We gratefully acknowledge support from the US-Israel BSF SP#2018-190, National Science Foundation (IOS165674), and National Institute of Health (1R01GM127872) to ACK, and the National Institute of Health (DC010809), National

Science Foundation (IOS1856237, IOS2102891), and support from the Whitney Laboratory for Marine Biosciences to JCL.

Abstract (177/200)

Animals can evolve dramatic sensory functions in response to environmental constraints, but little is known about the neural mechanisms underlying these changes. The Mexican tetra, *Astyanax mexicanus,* is a leading model to study genetic, behavioral, and physiological evolution by comparing eyed surface populations and blind cave populations. We compared neurophysiological responses of posterior lateral line afferent neurons and motor neurons across *A. mexicanus* populations to reveal how shifts in sensory function may shape behavioral diversity. These studies indicate differences in intrinsic afferent signaling and gain control across populations. Elevated endogenous afferent activity identified a lower response threshold in the lateral line of blind cavefish relative to surface fish leading to increased evoked potentials during hair cell deflection in cavefish.. We next measured the effect of inhibitory corollary discharges from hindbrain efferent neurons onto afferents during locomotion. We discovered that three independently-derived cavefish populations have evolved persistent afferent activity during locomotion, suggesting for the first time that partial loss of function in the efferent system can be an evolutionary mechanism for neural adaptation of a vertebrate sensory system.

Introduction

Our understanding of the sensory systems and behavior of animals is challenging to contextualize within the framework of evolution. Anatomical comparisons between species have allowed us to infer sensory capabilities, but this approach cannot directly reveal neural function. Discovery of neural mechanisms that underlie behavior are often constrained to a limited number of model species (Jourjine & Hoekstra, 2021). Like morphology, neural circuits can adapt to the environment. Of these, many circuits are sensory and regulate essential behaviors such as foraging, navigation, and escapes (Blin et al., 2018; Hoke et al., 2012; Hüppop, 1987; Paz et al., 2020).

The Mexican blind cavefish, *Astyanax mexicanus,* is a powerful model to understand the evolution of physiological and molecular traits that contribute to behaviors such as sleep (Duboué et al., 2011; J. B. Jaggard et al., 2018) and prey capture (Lloyd et al., 2018; Yoshizawa et al., 2014). *Astyanax mexicanus* exists in two morphs; 1) eyed surface-dwelling populations and 2) blind cave populations. There are at least 30 independently evolved cavefish populations in the caves of the Sierra de El Abra region of Northeast Mexico (Espinasa et al., 2018; Herman et al., 2018; McGaugh et al., 2020; RW Mitchell et al., 1997). *Astyanax mexicanus* populations are interfertile, and this attribute has allowed investigators to demonstrate independent convergence of numerous behavioral, developmental, and physiological traits (Chin et al., 2018; Kowalko, 2020; Riddle et al., 2018; Stockdale et al., 2018; Varatharasan et al., 2009). Our goal is to apply a neurophysiological approach across multiple *A. mexicanus* populations to examine the functional evolution of the lateral line sensory system.

The mechanoreceptive hair cells of the lateral line system detects fluid motion relative to the body and play an important role in essential behaviors (McHenry et al., 2009; Mekdara et al., 2018; Olszewski et al., 2012; Oteiza et al., 2017; Stewart et al., 2013). Cavefish have

evolved anatomical enhancements of the lateral line, presumably to compensate for the loss of vision (Kowalko, 2020; McGaugh et al., 2020; Teyke, 1990; Yoshizawa et al., 2012). These anatomical alterations have been linked to substantial changes in behavior (Lloyd et al., 2018; Yoshizawa et al., 2010). However, almost nothing is known about physiological changes that accompany evolution, despite the fact that the response of peripheral senses to environmental change has been well documented (Kelley et al., 2018; McBride, 2007).

Endogenous depolarizations within sensory cells are transmitted to afferent neurons (hereafter "afferents") as spontaneous action potentials (hereafter "spikes"), and are essential for maintaining a state of responsiveness and sensitivity (Kiang, 1965; Manley & Robertson, 1976). For example, the spontaneous spikes from auditory hair cells have been shown to enable precise encoding of much higher frequencies (Köppl, 1997). Here, we suggest a similar underlying mechanism, though the correlation of spontaneous activity to sensitivity in the lateral line awaits empirical evidence. In the lateral line, spontaneous depolarizing currents within the hair cell maintain a resting potential within the critical activation range of channels. This range is required to ensure transmitter release; thus these currents decrease the detection threshold of the system (Trapani & Nicolson, 2011). Spontaneous afferent activity is an established and reliable target for probing the neurophysiological basis of sensitivity across taxa (Hedwig, 2006; Krasne & Bryan, 1973; Mohr et al., 2003). Here, we use spontaneous afferent activity as an entry point into understanding the neural mechanism underlying lateral line function in cavefish.

Another important mechanism that determines lateral line sensitivity is an inhibitory feedback effect of the efferent system during swimming. Feedback mechanisms in general sculpt sensory systems in important ways; for example, by changing detection thresholds by altering the transmission frequency of afferent spikes (Crapse & Sommer, 2008; Straka et al., 2018). The efferent system of hair cells in particular has repeatedly evolved to modulate

sensory processing (Köppl, 2011). More specifically, hindbrain efferent neurons (hereafter "efferents") issue predictive signals that transmit in parallel to locomotor commands, termed corollary discharge (CD). CDs inhibit afferent activity to mitigate sensor fatigue that can result from self-generated stimuli (Russell & Roberts, 1972). CD is an important mechanism for sensitivity enhancement but has rarely been implicated for ecologically-relevant behaviors. For example, active-flow sensing by cavefish depends on detecting reafferent signals while swimming (Tan et al., 2011). Increased reliance on self-generated fluid motion (Odstrcil et al., 2021; Patton et al., 2010; Teyke, 1985) is divergent from our current understanding of the CD's role in predictive motor signaling in the lateral line (Lunsford et al., 2019; Pichler & Lagnado, 2020).

For the first time, we identify a neurophysiological mechanism that has convergently evolved across *A. mexicanus* populations to increase hair cell sensitivity after eye loss. By investigating how differences in afferent and efferent signaling contribute to sensory enhancement in a comparative model, we provide insight into a potentially ubiquitous mechanism for sensory evolution.

Results

Neuromasts of surface fish and Pachón cavefish larvae (6 days post fertilization; dpf) were labeled via 2-[4- (Dimethylamino)styryl]-1-ethylpyridinium iodide (DASPEI) staining and subsequently imaged (Figure 1B-C). Anterior lateral line neuromasts had previously been shown to differ in quantities and morphology as early as 2 months post fertilization between surface and cave fish (Yoshizawa et al., 2010). Here we show that Pachón cavefish exhibit this significant increase in anterior neuromast quantity as early as 6 dpf ($p < 0.01$, $t = 3.168$, $df = 29$; Figure 1D). In contrast, both populations exhibit a similar number of posterior lateral line neuromasts ($p = 0.77$, $U = 111.5$; Figure 1E). Neuromasts along the posterior lateral line

were comprised of similar quantities of hair cells across blind (n = 11) and surface morphs (n = 9; p = 0.09; Figure 1F). No significant interaction was detected between the effects of population and age (5-7 dpf; $F_{2,72}$ = 2.96, p = 0.06; Figure 1G). We exclusively probed the posterior lateral line afferent neurons to establish whether sensory systems that are anatomically similar exhibit neurophysiological differences that contribute to enhanced sensitivity.

To examine the physiological basis of differences in lateral line function across surface and cavefish we used extracellular lateral line recordings adapted from protocols used in zebrafish (Figure 2 A-B). Extracellular recordings of posterior lateral line afferents revealed intrinsic spontaneous activity was higher in Pachón cavefish (18.6 ± 0.2 Hz) while the animal was at rest, relative to surface fish (12.4 ± 0.3 Hz; p < 0.01, t = 15.97, df = 5,795; Figure 2C). Single neuromasts were then deflected and evoked activity was recorded from the connected afferent neuron (Figure 2 D-E). The neuromasts were stimulated at different frequencies (5-40 Hz) and a pairwise comparison of evoked afferent activity at 30 Hz revealed statistically elevated spike rates in Pachón cavefish (n = 12; 119.6 ± 16.6 Hz) relative to surface fish (n = 10; 73.2 ± 6.9 Hz; p = 0.03, t = 2.38, df = 18; Figure 2 F). Significantly elevated spike rates were also detected in response to a 40 Hz stimulus in Pachón cavefish (101.3 ± 13.6 Hz) relative to surface fish (52.3 ± 7.0 Hz; p < 0.01, t = 3.00, df = 18; Figure 2 F). Together these findings support spontaneous afferent activity as a reliable metric for estimating the sensitivity of the lateral line and reveal enhanced neural responses to hair cell deflection in cavefish.

We examined afferent signaling during motor commands in our paralyzed preparation which were denoted by bouts of fictive swimming (hereafter swimming). Swim bouts of longer duration were observed in surface fish (357 ± 5 ms; n = 3,167 swim bouts) when compared to Pachón cavefish (264 ± 4 ms; n = 2,612 swim bouts; p < 0.01, t-stat = 15.2, df = 5777).

Instantaneous afferent spike rate demonstrates substantial decreases during swimming in surface fish and little effect in Pachón cavefish (Figure 3 A-B). We quantified and compared spike rates during swimming relative to the pre-swim period to examine patterns of the inhibitory effect between populations. During most surface fish swim bouts there was a reduction in afferent activity (n = 1,966/2,291, 85.8%), many of which resulted in complete quiescence of transmissions (n = 1,112/2,291, 48.5%). Conversely, afferent activity partially reduced during many swim bouts in Pachón cavefish (n = 1,303/2,439, 53.4%), but very few instances led to complete inhibition (n = 275/2,439, 11.3%). The distributions of relative spike rates during swimming reveal surface fish have a higher likelihood of experiencing no afferent activity during swimming while cavefish experience afferent activity during swimming similar to that of pre-swim activity levels (Figure 3 C). Therefore, surface fish experience significantly higher levels of inhibition (68.5 ± 0.01%) compared to cavefish (28.9 ± 0.01%; $p < 0.01$, $t = 36.5$, $df = 4449$; Figure 3 D). Surface fish demonstrate lateral line inhibition during swimming comparable to other fishes with intact visual systems (Flock & Russell, 1973; Lunsford et al., 2019; Pichler & Lagnado, 2020; Russell & Roberts, 1972) suggesting cavefish have evolved a unique functional phenotype for sensory gain control.

We imaged hindbrain cholinergic efferent neurons to determine anatomical and functional connectivity. Between populations, backfilled efferents revealed similar soma quantities (surface: 2.4 ± 0.3; cave: 3.2 ± 0.5; $p = 0.2$, $t = 1.36$, $df = 18$) and size (surface: 62.1 ± 3.6 μm^2; cave: 70.9 ± 4.5 μm^2; $p = 0.1$, $t = 1.50$, $df = 51$; Figure 4 A-C). From electrophysiological recordings, we observed average spike rates during and prior to a swim were not positively correlated in control surface fish ($r^2 = 0.15$, $F_{1,13} = 2.3$, $p = 0.2$), but the slope of the line indicates a fractional suppression of 78% that is significantly less than unity (slope 0.1, confidence interval (CI): -0.2-0.4; Figure 4 Di). In the efferent ablated surface fish, the spike rates during swimming intervals was indistinguishable from those during non-

swimming intervals (slope 1.2, CI = -0.1-2.4) showing no detectable inhibitory effect. While swimming, surface fish without functioning efferent neurons demonstrated a signaling phenotype similar to both intact cavefish (slope 0.88, CI = -0.5-2.2) and cavefish with ablated efferents (slope 0.9, CI = 0.1-1.8; Figure 4 Dii). Therefore, putative cholinergic hindbrain efferents are necessary for afferent inhibition in surface fish, but do not demonstrate modulatory control of afferents in cavefish.

We compared pre-swim and swim spike rates across populations and treatments to determine efferent contribution to inhibition (Figure 4 E). We found significant differences in afferent activity among pre-swim and swim intervals ($F_{7,40}$ = 7.6, $p < 0.01$; Figure 4 F). Surface fish afferent spike rates during swimming (3.9 ± 0.1 Hz) were 71% lower than the immediate pre-swim period in control fish (13.7 ± 0.2 Hz; Tukey's post hoc test, $p < 0.01$). Post-swim spike rate (13. 7 ± 0.3 Hz) recovered to pre-swim spike rate. In control Pachón cavefish, we observed some decrease in afferent spike rate during swimming (16.8 ± 0.2 Hz) but it was not statistically discriminated from pre-swim (20.5 ± 0.2 Hz; Tukey's post hoc test, $p = 0.94$). Efferent ablation in surface fish resulted in afferent activity during swimming (17.4 ± 0.3 Hz) to increase to pre-
swim levels (20.7 ± 0.3 Hz; Tukey's post hoc test, $p = 0.99$). Ablated surface fish also demonstrated spike dynamics during swimming comparable to ablated and control cavefish (Pachón ablated, pre-swim: 18.6 ± 0.3 Hz; Pachón ablated, swimming: 14.7 ± 0.3 Hz). These findings indicate that efferents are necessary for inhibition of afferents during swimming in surface fish.

We compared lateral line activity between three different cave populations (Figure 5 A); the Tinaja and Pachón populations, which are derived from similarly timed colonization events, and the Molino population that is derived from a more recent colonization event (Bradic et al., 2012; Dowling et al., 2002; Herman et al., 2018). Blind cavefish populations

exhibited similar spontaneous spike rates across populations ($F_{2,17}$ = 0.68, p = 0.52), and swimming showed little effect on lateral line activity across blind cavefish populations (Figure 5 B). We observed a minor decrease in afferent spike rates across cavefish populations and the relative change (i.e. inhibition) was similar in Pachón and Tinaja (Tukey's post hoc test; Pachón: 0.28 ± 0.01; Tinaja: 0.32 ± 0.02; Figure 5 C). Molino demonstrated an intermediate phenotype compared to Pachón and Tinaja (Tukey's post hoc test; Molino: 0.23 ± 0.01; $p < 0.01$). The Molino population (new lineage) is most distantly related to the Pachón and Tinaja populations (old lineage), originating from a more recent surface fish colonization of caves thus providing phylogenetic evidence that
coincides with statistically similar groupings (Herman et al., 2018). We examined the correlation between non-swimming and swimming spike rates across cave populations to determine whether the inhibitory effect was significant. Spike rates during swimming and pre-swim intervals were positively correlated in all cave populations, and afferent spike rates during swimming were not statistically distinguishable from unity across populations (Pachón: slope = 0.88, CI = -0.5 – 2.2; Tinaja: slope = 1.03, CI = -0.2 - 2.2; Molino: slope = 1.02, CI = 0.8 - 1.2; Figure 5 D), indicating there was no significant decrease in afferent activity during swimming within blind cavefish populations.

Discussion

Our principal findings indicate elevated afferent spike activity and an increased responsiveness to hair cell deflection in cavefish. The increased afferent activity in cavefish is a likely consequence of eye-loss, which has robust effects on other physiological systems (Duboué et al., 2011; Varatharasan et al., 2009). Heightened lateral line sensitivity in adults has been previously attributed to increased neuromast density in the anterior lateral line (ALL) as well as increased hair cell quantities per neuromast (J. Jaggard et al., 2017; Lloyd et al., 2018; McHenry et al., 2008; Patton et al., 2010; Teyke, 1990; Yoffe et al., 2020, 2020;

228 Yoshizawa et al., 2010). These differences do not exist in the posterior lateral line at the
229 larval stage, allowing us a unique opportunity to investigate the neural mechanisms that can
230 enhance flow sensing in a strong model for evolution. Our discovery of increased
231 spontaneous activity that contributes to the enhanced evoked responses in cavefish is a
232 powerful addition for flow sensing, and we predict that this in combination with the increased
233 number of neuromasts in the ALL (Yoshizawa et al., 2010) is what ultimately enables
234 cavefish to perform active flow sensing.

235 Higher spontaneous activity is one of two mechanisms that are responsible for higher
236 lateral line sensitivity. The other involves the inhibitory effects of the efferent system during
237 swimming, a feedback mechanism that is conserved across the diversity of fishes (Flock &
238 Russell, 1973; Lunsford et al., 2019; J. Montgomery et al., 1996; J. C. Montgomery &
239 Bodznick, 1994; Roberts & Russell, 1972; Tricas & Highstein, 1991). This is true in
240 swimming surface fish but not in cavefish. We found that three blind populations of cavefish
241 (i.e. Pachón, Molino, Tinaja) have repeatedly lost the capability for efferent modulation
242 during swimming. When one considers that lateral line efferent activity can be driven by
243 direct inputs from the visual system in zebrafish (Reinig et al., 2017), it seems possible that
244 eye degeneration induces the loss of efferent function. This interpretation is consistent with
245 the idea that lateral line efferents are thought to have undergone regressive loss before in the
246 ancestral lamprey and hagfish (Kishida et al., 1987; Köppl, 2011; Koyama et al., 1990), both
247 of which are nearly or completely blind during development (Dickson & Collard, 1979;
248 Fernholm & Holmberg, 1975). However, our results illustrate that cholinergic efferent system
249 is still present in cavefish, having lost functionality rather than disappearing (the efferent
250 system is functional in surface fish). Exploring pre- and postsynaptic differences such as
251 acetylcholine release or the density of nicotinic acetylcholine receptors (nAChR) may explain

252 the reduced inhibitory efficacy and reveal molecular targets that could disrupt efferent
253 function over the course of evolution (Dawkins et al., 2005).

254 Our demonstration of CD inactivity in cavefish provides an alternative mechanism by
255 which evolution can enhance sensitivity, one that proceeds by decreasing inhibition rather
256 than augmenting sensor morphology or density (Yamamoto et al., 2009; Yoshizawa et al.,
257 2010, 2014). The impact of increasing sensitivity through a lack of inhibition is apparent
258 during active-flow sensing in adult *A. mexicanus*. Active-flow sensing occurs during
259 swimming and involves using the reflection of self-generated flow fields (Bleckmann et al.,
260 1991) to follow walls (Patton et al., 2010), avoid obstacles (Teyke, 1985; Windsor et al.,
261 2008), and discrimination between shapes (De Perera, 2004; Hassan, 1989; Von
262 Campenhausen et al., 1981). The repeated loss of inhibition across populations at the larval
263 stage suggests that selection may act early in development on the efferent over afferent
264 systems. Future experiments may test this hypothesis in adults, though it seems likely that
265 this phenomenon would be preserved and only elaborated on throughout ontogeny, rather
266 than reconfigured. Cavefish swim by using different body motions than surface fish. This
267 finding has been interpreted as a mechanism to enhance wall following, which occurs when
268 the bow wake of a swimming cavefish is reflected off of a solid surface and then detected
269 (Patton et al., 2010; Sharma et al., 2009). Altered swimming kinematics is also thought to
270 have arisen from a general increase in sensitivity to flow (Tan et al., 2011; Windsor et al.,
271 2008). Our results provide an alternate suggestion; the lack of efferent function in cavefish
272 precludes the sensory feedback necessary for sensing self-movement and body position in
273 water (proprioception). Corollary discharge, a parallel motor command that decreases the
274 afferent activity of fishes when swimming, has recently been found to play a critical role in
275 swimming efficiency by enabling the tracking of the traveling body wave during undulation
276 (Skandalis et al., 2021). We hypothesize that the evolved loss of efferent function that

enables cavefish to successfully avoid collisions in subterranean habitats is likely favored over optimizing swimming efficiency (Nakamura, 1997; Uysal et al., 2010). We predict that loss of efferent function will be found in other blind hypogean species (Costa Sampaio et al., 2012) and that their respective surface populations will possess intact efferent functionality, as we have found in *A. mexicanus.* Neurophysiological recordings across a wider diversity of species would provide valuable insight into how efferent function may be sculpted by environmental selection and phylogenetic membership.

By employing neurophysiological approaches in the lateral line system of *A. mexicanus* for the first time, we show that elevated lateral line afferent activity and loss of efferent function have repeatedly evolved together across cavefish populations. Our findings come at a time when genetic tools in *A. mexicanus* enable brain-wide imaging and gene-editing based screening to identify candidate neural circuits and genes critical in the evolution of sensory systems (Jaggard et al., 2020; Warren et al., 2021). Going forward, applying genetic and electrophysiological tools in well-characterized neural circuits promises to inform our understanding of the evolution of neural systems and behavior more broadly.

Figure Captions

Figure 1. Surface fish and cavefish lateral lines are anatomically similar in early development. Illustration (not to scale) of the canonical circuit of lateral line function depicting the neuromast (blue) comprised of mechanoreceptive hair cells that are innervated by ascending afferent neurons (green) that collect into the posterior lateral line ganglion. Putative cholinergic efferent neurons (red) descend from the hindbrain and project onto neuromast hair cells (**A**). DASPEI staining of 6 dpf surface (**B**) and cavefish (**C**) show significantly different quantities of anterior lateral line neuromasts (**D**) and similar quantities of posterior neuromasts (**E**). Hair cells were labeled with a 30 min treatment of YO-PRO1

(green) and found to be of similar quantities between populations (**F**). Box-and-whisker plot representing number of hair cells per neuromast were indistinguishable across development (5-7 dpf; **G**). Error bars are ± SE.

Figure 2. Dynamics of spontaneous and evoked afferent neuron spike activity is elevated in cavefish. Extracellular recordings were made in posterior lateral line afferents where the neuromast densities and hair cell quantities were similar to resolve the differences observed in afferent activity between larval surface fish (**A**) and Pachón cavefish (**B**) between 4-7 dpf. Number of occurrences and median intrinsic spike rates in both surface (blue; 12.4 Hz, n=10 fish) and Pachón (red; 18.6 Hz, n=5 fish) fish suggests that lateral line response thresholds in cavefish are lower than those of surface fish (**C).** Evoked afferent activity during stimulation of a single neuromast in surface fish (**D**) and cavefish (**E**) and peristimulus time histograms demonstrate elevated spike rate in cavefish. Evoked spike rate was stimulus frequency dependent and pairwise comparisons reveal significantly (open circles) elevated sensitivity in cavefish at 30 and 40 Hz (**F**). Error bars are ± SE.

Figure 3. Afferent spike rate decreases during swimming in surface fish but not cavefish. Simultaneous recordings from afferent neurons from the posterior lateral line afferent ganglion and ventral motor roots along the body in (**Ai**) surface fish and (**Bi**) Pachón cavefish. Afferent spike rate decreases at the onset of swimming (time = 0) in (**Aii**) surface fish while (**Bii**) Pachón cavefish spike rate remained relatively constant during swimming. Bars represent average swim duration for surface fish (357 ± 5 ms, n = 2,272 swims) and Pachón cavefish (264 ± 4 ms, n = 2,612 swims). **C.** Kernel density estimate of spike rate during swimming relative to the pre-swim interval in both surface fish (blue) and cavefish

(red). **D.** Surface fish experience greater levels of inhibition during swimming than cavefish. Significance level $p < 0.001$ indicated by '***'. Error bars are ± SE.

Figure 4. Efferent neurons are necessary for inhibition observed in afferents during swimming in surface fish but not cavefish. A. Backfilled hindbrain cholinergic efferent neurons were present in comparable numbers (2-3 cells) in both surface fish (n = 14) and cavefish (n = 6). **Bi.** Efferent soma size in surface (blue) and cavefish (red) is similar in both populations (**ii**). **C.** Efferent cell bodies were identified by backfilling rhodamine through posterior lateral line neuromasts in both surface fish (**i**) and cavefish (**ii**) and were ablated with a 30-s UV pulse. Scale bar: 20 μm. **D.** The line of best fit of spike rates before compared to during the swim significantly excludes unity in non-ablated, control surface fish (circle), but not in ablated surface fish (square), implying spike rate suppression in the former but not the latter (**i**). The slope of the line for control fish suggests the inhibition is not correlated to the spontaneous afferent activity preceding the swim. The line of best fit of Pachón cavefish pre-swim and swim spike rates did not exclude unity in both control (circle) and ablated (square) treatments (**ii**). Dashed line indicates the line of unity, corresponding to no average difference of spike rate during swimming. **E.** Instantaneous spike rates of Pachón cavefish were unaffected by ablating the lateral line whereas the inhibitory effect was eliminated in ablated surface fish. Time is relative to the onset of motor activity. **F.** Surface fish (blue) display reduced spike rates during swimming compared to before swimming in control fish. Pachón cavefish (red) did not display reduced spike rate during swimming in neither control nor ablated treatments. Ablated surface individuals also did not display reduced spike rate during swimming resulting in a signaling phenotype comparable to cavefish. Groupings of statistical similarity are denoted by 'a' and 'b', whereas a is significantly different from b. All error bars represent ± SE.

Figure 5. Enhanced lateral line sensitivity during swimming convergently evolved across three blind populations. A. Molino cave populations (pink; New Lineage) have evolved more recently relative to Pachón (red) and Tinaja (purple; Old Lineage) cave populations. Lineage delineations inferred from phylogenetic data (Herman et al. 2018). **B.** Mean spontaneous afferent spike rate remains constant at the onset of fictive swimming (time = 0) in Pachón (n = 5), Molino (n = 8), and Tinaja (n = 5) populations. Bar represents average swim duration for Pachón (0.27 sec, n = 2,429 swim bouts), Molino (0.42 sec, n = 1,474 swim bouts), and Tinaja (0.35 sec, n = 464). **C.** Percent change in spike rate from pre-swim to swim intervals (i.e. inhibition) was small, but significantly different between blind cave populations. Post-hoc Tukey test revealed that Molino cavefish experienced significantly less reduction in spike rate when compared to Pachón and Tinaja populations. Statistically similar groups are indicated by 'a' and 'b'. **D.** The line of best fit of pre-swim and swim spike rates does not significantly exclude unity in any of the blind cavefish populations implying there is no detectable inhibitory effect. Dashed line indicates the line of unity, corresponding to no average difference of spike rate during swimming. All values represent mean ± SE.

Supplementary File 1. Data collected from electrophysiology recordings and hair cell imaging. Afferent spike rate during motor-inactivity, fictive swimming, and neuromast deflection. Data includes information related to the parameters of fictive swim bouts (i.e. tail-beat frequency, swim duration, and duty-cycle) as well as stimulus frequency associated with evoked activity. Imaging data denotes the population (Pachón or surface), age, and neuromast identity associated with each hair cell count.

Materials and Methods

375 *Animals*: Fish were progeny of pure-bred stocks originally collected in Mexico
376 (Duboué et al., 2011) that have been maintained at the Florida Atlantic University core
377 facilities. Larvae were raised in 10% Hank's solution (137 mM NaCl, 5.4 mM KCl, 0.25 mM
378 Na_2HPO_4, 0.44 mM KH_2PO_4, 1.3 mM $CaCl_2$, 1.0 mM $MgSO_4$, 4.2 mM $NaHCO_4$; pH 7.3) at
379 26°C. All experiments were performed according to protocols approved by the University of
380 Florida or Florida Atlantic University Institutional Animal Care and Use Committee
381 (IACUC201603267, IACUC202200000056). Animal health was assessed by monitoring
382 blood flow throughout each experiment.
383 *Neuromast imaging*: To assess neuromast quantities, larvae aged six dpf were submerged in 5
384 μg/ml DASPEI dissolved in embryo medium for 15 minutes as previously described (Van
385 Trump et al., 2010). Larvae were then transferred to ice-cold water for 30-45 seconds then
386 immersed in 8% methylcellulose for imaging. Images were taken using a Nikon DS-Qi2
387 monochrome microscope camera mounted on a Nikon SMZ25 Stereo microscope (Nikon;
388 Tokyo, Japan). Neuromasts innervated by posterior lateral line afferents and anterior lateral
389 line afferents were tabulated separately. To image hair cells that comprise each neuromast,
390 larvae (5-7 dpf) were immersed in 2 μM YO-PRO1 (Invitrogen; Y3603) in embryo media for
391 30 min, rinsed three times in embryo media (Santos et al., 2006). Larvae were then embedded
392 on their sides in low-melting point-1.6% agarose and imaged on a confocal microscope
393 (Leica TCS SP5, 63x/1.2 water immersion, 200 Hz, emission: 644 nm - 698 nm). Images
394 were processed on ImageJ (v1.48; U. S. National Institutes of Health, Bethesda, MD).

395 *Electrophysiology*: Prior to recordings, *A. mexicanus* larvae (4-7 dpf) were paralyzed
396 using 0.1% α-bungarotoxin (Lunsford & Liao, 2021). Once paralyzed, larvae were then
397 transferred into extracellular solution (134 mM NaCl, 2.9 mM KCl, 1.2 mM $MgCl_2$, 2.1 mM
398 $CaCl_2$, 10 mM glucose, 10 mM HEPES buffer; pH 7.8, adjusted with NaOH) and pinned with

399 etched tungsten pins through their dorsal notochord and otic vesicle into a Sylgard-bottom
400 dish.

401 Multiunit extracellular recordings of the posterior lateral line afferent ganglion were
402 made in surface fish (n = 10) and Pachón cave fish (n = 5). Prior to recording from the
403 afferent neurons, a bore pipette was used to break through the skin to expose the afferent
404 soma. Recording electrodes (~30 μm tip diameter) were pulled from borosilicate glass (model
405 G150F-3, inner diameter: 0.86, outer diameter: 1.50; Warner Instruments, Hamden, CT) on a
406 model P-97 Flaming/Brown micropipette puller (Sutter Instruments, Novato, CA) and filled
407 with extracellular solution. Once contact with afferent somata was achieved, gentle negative
408 pressure was applied (20-50 mmHg; pneumatic transducer tester, model DPM1B, Fluke
409 Biomedical Instruments, Everett, WA). Pressure was adjusted to atmospheric (0 mmHg) once
410 a stable recording was achieved. Simultaneously, ventral root (VR) recordings were made
411 through the skin (Masino & Fetcho, 2005) to detect voluntary fictive swimming. To record
412 response properties from afferent neurons during neuromast deflection we systematically
413 probed neuromasts starting at D1 and continued down the body until stereotypical evoked
414 potentials were detected (Levi et al., 2015). The sinusoidal stimulus was driven using a
415 single-axis piezo stimulator (30V300, Piezosystem Jena, Hopedale, Massachusetts, USA).
416 The stimulus probe was formed by melting the tip of a small diameter (~ 2 μm) recording
417 electrode on a MF-830 microforge (Narishige International, Amityville, New York, USA)
418 and the probe tip was positioned approximately 50 μm anterior to the cupula at kinocilia-tip
419 height. Stimulation occurred at 5 Hz, 10 Hz, 20 Hz, 30 Hz, and 40 Hz which encompasses
420 frequency ranges at the lower limit of tail beats (5-10 Hz) and typical range of tail-beat
421 during free swimming (20-40 Hz)(Mirat et al., 2013). The stimulus period lasted for 1
422 second with 4 seconds at rest to allow for recovery and was repeated for each frequency for
423 60 sweeps. Care was taken to avoid any contact between the probe and the cupula which can

alter the response (Levi et al., 2015). All recordings were sampled at 20 kHz and amplified with a gain of 1000 in Axoclamp 700B, digitized with Digidata 1440A and saved in pClamp10 (Molecular Devices).

All recordings were analyzed in Matlab (vR2019b) using custom written scripts. Both spontaneous afferent spikes and swimming motor activity identified using a combination of spike parameters previously described (Lunsford et al., 2019). Afferent neuron activity within a time interval equal to the subsequent fictive swim bout, hereafter termed "pre-swim", was quantified and compared to afferent activity during swimming to measure relative changes in spontaneous firing.

Efferent Ablations: Hindbrain efferent neurons were backfilled with tetramethylrhodamine (TRITC, 3 kDa; Molecular Probes, Eugene, OR). *A. mexicanus* larvae (4 dpf) were anesthetized in MS-222 (Tricaine, Western Chemical Inc. Ferndale, WA) and embedded in agar. To selectively label the hindbrain cholinergic efferent neurons, we systematically electroporated (Axoporator 800A Single Cell Electroporator, Axon CNS Systems, Molecular Devices LLC, San Jose, CA) TRITC into the efferent terminals that innervate the D1, D2, L1, and L2 neuromasts of the lateral line in surface fish (n = 14) and Pachón cavefish (n = 7; Figure 4 Ci). Electroporation does not ensure labelling of all efferent neurons so we standardized parameters (30 V, 50 Hz, 500 ms, square pulse) and targeted the same neuromasts across populations to minimize variation in labelling efficacy. Larvae were then gently freed from the agar and allowed to swim freely and recover overnight. Larvae (5 dpf) were then paralyzed via α-bungarotoxin immersion, remounted in agar dorsal surface down, and imaged on a Leica SP5 confocal microscope (Leica Microsystems, Wetzlar, Germany). Efferent soma size and quantity was measured within identified TRITC-labelled cells in ImageJ (v1.48; U. S. National Institutes of Health, Bethesda, MD). To perform targeted ablations of surface fish (n = 5) and cavefish (n = 6) efferent neurons, a near-

ultraviolet laser was focused at a depth corresponding to the maximum fluorescence intensity of each soma, to ensure we were targeting its centre. We applied the FRAP Wizard tool in Leica application software to target individual cells. We ablated target cells with a 30 s exposure to the near-ultraviolet laser line (458 nm), and successful targeting was confirmed by quenching of the backfilled dye. This method has been successfully applied and validated in similar systems (Liu & Fetcho, 1999; Soustelle et al., 2008). Fish were again freed from agar and allowed to swim freely and recover overnight. Electrophysiological recordings were performed on ablated surface fish (n = 4) and cavefish (n = 5) at 6 dpf to simultaneously monitor afferent activity and motor activity.

Statistical analysis: Neuromast data were analyzed using GraphPad Prism 8.4.3. Normality was assessed via Shapiro-Wilk test. Anterior lateral line neuromast count data were found to be normally distributed. Anterior lateral line neuromast quantities in surface and cave larvae were compared using an unpaired t-test. Posterior lateral line neuromast count was found to not be normally distributed and was subsequently analyzed via Mann-Whitney U-test Neuromast hair cell data were analyzed using MatLab (v2019b). Surface and cavefish hair cell counts per neuromast compared using an unpaired two-way t-test.

Analyses of electrophysiological data (Supplementary File 1) were performed using custom written models in the R language (R development core team, vR2016b) using packages car, visreg, reshape2, plyr, dplyr, ggplot2, gridExtra, minpack.lm, nlstools, investr, and cowplot (Auguie et al., 2017; Baty et al., 2015; Breheny & Burchett, 2017; Fox & Weisberg, 2018; Wickham, 2007, 2009; Wickham et al., 2019; Wilke, 2019) and Matlab (v2019b). Spontaneous afferent spike rate was calculated by taking the number of spikes over the duration of time where the larva was inactive and the neuromast was not being stimulated. Instantaneous afferent spike rate was calculated using a moving average filter and a 100 ms sampling window. Evoked afferent spike rate was calculated by taking the number of spikes

474 over the duration of the stimulus period (1 s). Pre-swim and swim spike rate were calculated
475 by taking the number of spikes within the respective period over its duration. Pre-swim
476 periods of inactivity made it challenging to interpret changes in afferent activity, so we
477 restricted the dataset to only include swim bouts that were preceded by a minimum of one
478 afferent spike within the pre-swim interval (surface = 2,291 swim bouts; Pachón = 2,429
479 swim bouts; Molino = 1.474 swim bouts; Tinaja = 464 swim bouts). Swim frequency was
480 calculated by taking the number of bursts within a swim bout over the duration of the swim
481 bout. Relative spike rate was calculated by taking the swim spike rate over the pre-swim
482 spike rate. All variables were averaged for each individual fish. The precision of estimates for
483 each individual is a function of the number of swims, so we analyzed variable relationships
484 using weighted regressions, with individual weights equal to the square root of the number of
485 swims. We log transformed variables in which the mean and the variance were correlated. To
486 quantify the inhibition of the afferent spike frequency during swimming we tested for a
487 significant difference in afferent spike frequency during swimming as compared to non-
488 swimming periods using a paired sample student's t-test.
489 Differences in afferent spike rates between the periods of interest (pre-swim and swim)
490 across populations and treatments were tested by N-way analysis of variance (ANOVA)
491 followed by Tukey's post-hoc test to detect significant differences in spike rates between
492 swim periods or treatments. Linear models were used to detect relationships between spike
493 rate during swimming and other independent variables (e.g. spike rate pre-swim). Data is
494 shown throughout the manuscript as mean ± standard error. Statistical significance is reported
495 at $\alpha = 0.05$.
496

References

Auguie, B., Antonov, A., & Auguie, M. B. (2017). Package 'gridExtra.' *Miscellaneous Functions for "Grid" Graphics*.

Baty, F., Ritz, C., Charles, S., Brutsche, M., Flandrois, J.-P., & Delignette-Muller, M.-L. (2015). A toolbox for nonlinear regression in R: The package nlstools. *Journal of Statistical Software*, *66*(5), 1–21.

Bleckmann, H., Breithaupt, T., Blickhan, R., & Tautz, J. (1991). The time course and frequency content of hydrodynamic events caused by moving fish, frogs, and crustaceans. *Journal of Comparative Physiology A*, *168*(6), 749–757.

Blin, M., Tine, E., Meister, L., Elipot, Y., Bibliowicz, J., Espinasa, L., & Rétaux, S. (2018). Developmental evolution and developmental plasticity of the olfactory epithelium and olfactory skills in Mexican cavefish. *Developmental Biology*, *441*(2), 242–251.

Bradic, M., Beerli, P., García-de León, F. J., Esquivel-Bobadilla, S., & Borowsky, R. L. (2012). Gene flow and population structure in the Mexican blind cavefish complex (Astyanax mexicanus). *BMC Evolutionary Biology*, *12*(1), 9. https://doi.org/10.1186/1471-2148-12-9

Breheny, P., & Burchett, W. (2017). Visualization of regression models using visreg. *R J.*, *9*(2), 56.

Chin, J. S. R., Gassant, C. E., Amaral, P. M., Lloyd, E., Stahl, B. A., Jaggard, J. B., Keene, A. C., & Duboue, E. R. (2018). Convergence on reduced stress behavior in the Mexican blind cavefish. *Developmental Biology*, *441*(2), 319–327. https://doi.org/10.1016/j.ydbio.2018.05.009

Costa Sampaio, F. A., Pompeu, P. S., de Andrade e Santos, H., & Lopes Ferreira, R. (2012). Swimming performance of epigeal and hypogeal species of Characidae, with an emphasis on the troglobiotic Stygichthys typhlops Brittan & Böhlke, 1965. *International Journal of Speleology*, *41*(1), 2.

Crapse, T. B., & Sommer, M. A. (2008). Corollary discharge across the animal kingdom. *Nature Reviews. Neuroscience*, *9*(8), 587–600. https://doi.org/10.1038/nrn2457

Dawkins, R., Keller, S. L., & Sewell, W. F. (2005). Pharmacology of acetylcholine-mediated cell signaling in the lateral line organ following efferent stimulation. *Journal of Neurophysiology*, *93*(5), 2541–2551. https://doi.org/10.1152/jn.01283.2004

De Perera, T. B. (2004). Fish can encode order in their spatial map. *Proceedings of the Royal Society of London. Series B: Biological Sciences*, *271*(1553), 2131–2134.

Dickson, D. H., & Collard, T. R. (1979). Retinal development in the lamprey (Petromyzon marinus L.): Premetamorphic ammocoete eye. *American Journal of Anatomy*, *154*(3), 321–336.

Dowling, T. E., Martasian, D. P., & Jeffery, W. R. (2002). Evidence for multiple genetic forms with similar eyeless phenotypes in the blind cavefish, Astyanax mexicanus. *Molecular Biology and Evolution*, *19*(4), 446–455.

Duboué, E. R., Keene, A. C., & Borowsky, R. L. (2011). Evolutionary convergence on sleep loss in cavefish populations. *Current Biology*, *21*(8), 671–676. https://doi.org/10.1016/j.cub.2011.03.020

Espinasa, L., Legendre, L., Fumey, J., Blin, M., Rétaux, S., & Espinasa, M. (2018). A new cave locality for Astyanax cavefish in Sierra de El Abra, Mexico. *Subterranean Biology*, *26*, 39.

Fernholm, B., & Holmberg, K. (1975). The eyes in three genera of hagfish (Eptatretus, Paramyxine andMyxine)—A case of degenerative evolution. *Vision Research*, *15*(2), 253-IN4.

Flock, A., & Russell, I. J. (1973). The post-synaptic action of efferent fibres in the lateral line organ of the burbot Lota lota. *The Journal of Physiology*, *235*(3), 591–605. https://doi.org/10.1113/jphysiol.1973.sp010406

Fox, J., & Weisberg, S. (2018). *An R companion to applied regression*. Sage publications.

Hassan, E. S. (1989). Hydrodynamic imaging of the surroundings by the lateral line of the blind cave fish Anoptichthys jordani. In *The mechanosensory lateral line* (pp. 217–227). Springer.

Hedwig, B. (2006). Pulses, patterns and paths: Neurobiology of acoustic behaviour in crickets. *Journal of Comparative Physiology A*, *192*(7), 677–689. https://doi.org/10.1007/s00359-006-0115-8

Herman, A., Brandvain, Y., Weagley, J., Jeffery, W. R., Keene, A. C., Kono, T. J., Bilandžija, H., Borowsky, R., Espinasa, L., & O'Quin, K. (2018). The role of gene flow in rapid and repeated evolution of cave-related traits in Mexican tetra, Astyanax mexicanus. *Molecular Ecology*, *27*(22), 4397–4416.

Hoke, K., Schwartz, A., & Soares, D. (2012). Evolution of the fast start response in the cavefish Astyanax mexicanus. *Behavioral Ecology and Sociobiology*, *66*(8), 1157–1164.

Hüppop, K. (1987). Food-finding ability in cave fish (Astyanax fasciatus). *International Journal of Speleology*, *16*(1), 4.

Jaggard, J. B., Lloyd, E., Yuiska, A., Patch, A., Fily, Y., Kowalko, J. E., Appelbaum, L., Duboue, E. R., & Keene, A. C. (2020). Cavefish brain atlases reveal functional and anatomical convergence across independently evolved populations. *Science Advances*, *6*(38), eaba3126.

Jaggard, J. B., Stahl, B. A., Lloyd, E., Prober, D. A., Duboue, E. R., & Keene, A. C. (2018). Hypocretin underlies the evolution of sleep loss in the Mexican cavefish. *Elife*, *7*, e32637.

Jaggard, J., Robinson, B. G., Stahl, B. A., Oh, I., Masek, P., Yoshizawa, M., & Keene, A. C. (2017). The lateral line confers evolutionarily derived sleep loss in the Mexican cavefish. *Journal of Experimental Biology*, *220*(2), 284–293. https://doi.org/10.1242/jeb.145128

Jourjine, N., & Hoekstra, H. E. (2021). Expanding evolutionary neuroscience: Insights from comparing variation in behavior. *Neuron*.

Kelley, J. L., Chapuis, L., Davies, W. I. L., & Collin, S. P. (2018). Sensory System Responses to Human-Induced Environmental Change. *Frontiers in Ecology and Evolution*, *6*. https://doi.org/10.3389/fevo.2018.00095

Kiang, N. Y.-S. (1965). *Discharge patterns of single fibers in the cat's auditory nerve.* MASSACHUSETTS INST OF TECH CAMBRIDGE RESEARCH LAB OF ELECTRONICS.

Kishida, R., Goris, R. C., Nishizawa, H., Koyama, H., Kadota, T., & Amemiya, F. (1987). Primary neurons of the lateral line nerves and their central projections in hagfishes. *Journal of Comparative Neurology*, *264*(3), 303–310.

Köppl, C. (1997). Frequency tuning and spontaneous activity in the auditory nerve and cochlear nucleus magnocellularis of the barn owl Tyto alba. *Journal of Neurophysiology*, *77*(1), 364–377. https://doi.org/10.1152/jn.1997.77.1.364

Köppl, C. (2011). Evolution of the octavolateral efferent system. In *Auditory and vestibular efferents* (pp. 217–259). Springer.

Kowalko, J. (2020). Utilizing the blind cavefish Astyanax mexicanus to understand the genetic basis of behavioral evolution. *Journal of Experimental Biology*, *223*(jeb208835). https://doi.org/10.1242/jeb.208835

Koyama, H., Kishida, R., Goris, R. C., & Kusunoki, T. (1990). Organization of the primary projections of the lateral line nerves in the lamprey Lampetra japonica. *Journal of Comparative Neurology*, *295*(2), 277–289.

Krasne, F. B., & Bryan, J. S. (1973). Habituation: Regulation through Presynaptic Inhibition. *Science*, *182*(4112), 590–592.

Levi, R., Akanyeti, O., Ballo, A., & Liao, J. C. (2015). Frequency response properties of primary afferent neurons in the posterior lateral line system of larval zebrafish. *Journal of Neurophysiology*, *113*(2), 657–668.

Liu, K. S., & Fetcho, J. R. (1999). Laser ablations reveal functional relationships of segmental hindbrain neurons in zebrafish. *Neuron*, *23*(2), 325–335.

Lloyd, E., Olive, C., Stahl, B. A., Jaggard, J. B., Amaral, P., Duboué, E. R., & Keene, A. C. (2018). Evolutionary shift towards lateral line dependent prey capture behavior in the blind Mexican cavefish. *Developmental Biology*, *441*(2), 328–337. https://doi.org/10.1016/j.ydbio.2018.04.027

Lunsford, E. T., & Liao, J. C. (2021). Activity of Posterior Lateral Line Afferent Neurons during Swimming in Zebrafish. *JoVE (Journal of Visualized Experiments)*, *168*, e62233. https://doi.org/10.3791/62233

Lunsford, E. T., Skandalis, D. A., & Liao, J. C. (2019). Efferent modulation of spontaneous lateral line activity during and after zebrafish motor commands. *Journal of Neurophysiology*, *122*(6), 2438–2448.

Manley, G. A., & Robertson, D. (1976). Analysis of spontaneous activity of auditory neurones in the spiral ganglion of the guinea-pig cochlea. *The Journal of Physiology*, *258*(2), 323–336. https://doi.org/10.1113/jphysiol.1976.sp011422

Masino, M. A., & Fetcho, J. R. (2005). Fictive swimming motor patterns in wild type and mutant larval zebrafish. *Journal of Neurophysiology*, *93*(6), 3177–3188. https://doi.org/10.1152/jn.01248.2004

McBride, C. S. (2007). Rapid evolution of smell and taste receptor genes during host specialization in Drosophila sechellia. *Proceedings of the National Academy of Sciences*, *104*(12), 4996–5001. https://doi.org/10.1073/pnas.0608424104

McGaugh, S. E., Kowalko, J. E., Duboué, E., Lewis, P., Franz-Odendaal, T. A., Rohner, N., Gross, J. B., & Keene, A. C. (2020). Dark world rises: The emergence of cavefish as a model for the study of evolution, development, behavior, and disease. *Journal of Experimental Zoology Part B: Molecular and Developmental Evolution*, *334*(7–8), 397–404. https://doi.org/10.1002/jez.b.22978

McHenry, M. J., Feitl, K. E., Strother, J. A., & Van Trump, W. J. (2009). Larval zebrafish rapidly sense the water flow of a predator's strike. *Biology Letters*, *5*(4), 477–479. https://doi.org/10.1098/rsbl.2009.0048

McHenry, M. J., Strother, J. A., & Van Netten, S. M. (2008). Mechanical filtering by the boundary layer and fluid–structure interaction in the superficial neuromast of the fish lateral line system. *Journal of Comparative Physiology A*, *194*(9), 795.

Mekdara, P. J., Schwalbe, M. A. B., Coughlin, L. L., & Tytell, E. D. (2018). The effects of lateral line ablation and regeneration in schooling giant danios. *The Journal of Experimental Biology*, *221*(Pt 8). https://doi.org/10.1242/jeb.175166

Mirat, O., Sternberg, J. R., Severi, K. E., & Wyart, C. (2013). ZebraZoom: An automated program for high-throughput behavioral analysis and categorization. *Frontiers in Neural Circuits*, *7*, 107. https://doi.org/10.3389/fncir.2013.00107

Mohr, C., Roberts, P. D., & Bell, C. C. (2003). The Mormyromast Region of the Mormyrid Electrosensory Lobe. I. Responses to Corollary Discharge and Electrosensory Stimuli. *Journal of Neurophysiology*, *90*(2), 1193–1210. https://doi.org/10.1152/jn.00211.2003

Montgomery, J., Bodznick, D., & Halstead, M. (1996). Hindbrain signal processing in the lateral line system of the dwarf scorpionfish Scopeana papillosus. *Journal of Experimental Biology*, *199*(4), 893–899.

Montgomery, J. C., & Bodznick, D. (1994). An adaptive filter that cancels self-induced noise in the electrosensory and lateral line mechanosensory systems of fish. *Neuroscience Letters*, *174*(2), 145–148. https://doi.org/10.1016/0304-3940(94)90007-8

Nakamura, T. (1997). Quantitative analysis of gait in the visually impaired. *Disability and Rehabilitation*, *19*(5), 194–197.

Odstrcil, I., Petkova, M. D., Haesemeyer, M., Boulanger-Weill, J., Nikitchenko, M., Gagnon, J. A., Oteiza, P., Schalek, R., Peleg, A., Portugues, R., Lichtman, J. W., & Engert, F. (2021). Functional and ultrastructural analysis of reafferent mechanosensation in larval zebrafish. *Current Biology: CB*, S0960-9822(21)01530-X. https://doi.org/10.1016/j.cub.2021.11.007

Olszewski, J., Haehnel, M., Taguchi, M., & Liao, J. C. (2012). Zebrafish larvae exhibit rheotaxis and can escape a continuous suction source using their lateral line. *PloS One*, *7*(5), e36661. https://doi.org/10.1371/journal.pone.0036661

639 Oteiza, P., Odstrcil, I., Lauder, G., Portugues, R., & Engert, F. (2017). A novel mechanism for
640 mechanosensory-based rheotaxis in larval zebrafish. *Nature*, *547*(7664), 445–448.

641 Patton, P., Windsor, S., & Coombs, S. (2010). Active wall following by Mexican blind cavefish
642 (Astyanax mexicanus). *Journal of Comparative Physiology A*, *196*(11), 853–867.

643 Paz, A., McDole, B., Kowalko, J. E., Duboue, E. R., & Keene, A. C. (2020). Evolution of the acoustic
644 startle response of Mexican cavefish. *Journal of Experimental Zoology Part B: Molecular and*
645 *Developmental Evolution*, *334*(7–8), 474–485.

646 Pichler, P., & Lagnado, L. (2020). Motor Behavior Selectively Inhibits Hair Cells Activated by Forward
647 Motion in the Lateral Line of Zebrafish. *Current Biology*, *30*(1), 150-157.e3.
648 https://doi.org/10.1016/j.cub.2019.11.020

649 Reinig, S., Driever, W., & Arrenberg, A. B. (2017). The descending diencephalic dopamine system is
650 tuned to sensory stimuli. *Current Biology*, *27*(3), 318–333.

651 Riddle, M. R., Aspiras, A. C., Gaudenz, K., Peuß, R., Sung, J. Y., Martineau, B., Peavey, M., Box, A. C.,
652 Tabin, J. A., McGaugh, S., Borowsky, R., Tabin, C. J., & Rohner, N. (2018). Insulin resistance in cavefish
653 as an adaptation to a nutrient-limited environment. *Nature*, *555*(7698), 647–651.
654 https://doi.org/10.1038/nature26136

655 Roberts, B. L., & Russell, I. J. (1972). The activity of lateral-line efferent neurones in stationary and
656 swimming dogfish. *The Journal of Experimental Biology*, *57*(2), 435–448.

657 Russell, I. J., & Roberts, B. L. (1972). Inhibition of Spontaneous Lateral-Line Activity by Efferent Nerve
658 Stimulation. *Journal of Experimental Biology*, *57*(1), 77–82.

659 RW Mitchell, Russell, W., & Elliot, W. (1997). Mexican eyeless characin fishes, genus Astyanax:
660 Environment, distribution, and evolution. *Texas Tech Press*.
661 https://scholar.google.com/scholar_lookup?title=Mexican%20eyeless%20characin%20fishes%2C%2
662 0genus%20Astyanax%3A%20environment%2C%20distribution%2C%20and%20evolution.%2C%20Sp
663 ecial%20publications%20the%20museum%20Texas%20Tech%20University&author=R.W.%20Mitche
664 ll&publication_year=1977

665 Santos, F., MacDonald, G., Rubel, E. W., & Raible, D. W. (2006). Lateral line hair cell maturation is a
666 determinant of aminoglycoside susceptibility in zebrafish (Danio rerio). *Hearing Research*, *213*(1–2),
667 25–33. https://doi.org/10.1016/j.heares.2005.12.009

668 Sharma, S., Coombs, S., Patton, P., & De Perera, T. B. (2009). The function of wall-following behaviors
669 in the Mexican blind cavefish and a sighted relative, the Mexican tetra (Astyanax). *Journal of*
670 *Comparative Physiology A*, *195*(3), 225–240.

671 Skandalis, D. A., Lunsford, E. T., & Liao, J. C. (2021). Corollary discharge enables proprioception from
672 lateral line sensory feedback. *PLoS Biology*, *19*(10), e3001420.
673 https://doi.org/10.1371/journal.pbio.3001420. https://doi.org/10.1371/journal.pbio.3001420

674 Soustelle, L., Aigouy, B., Asensio, M.-L., & Giangrande, A. (2008). UV laser mediated cell selective
675 destruction by confocal microscopy. *Neural Development*, *3*(1), 11. https://doi.org/10.1186/1749-
676 8104-3-11

677 Stewart, W. J., Cardenas, G. S., & McHenry, M. J. (2013). Zebrafish larvae evade predators by sensing
678 water flow. *The Journal of Experimental Biology*, *216*(Pt 3), 388–398.
679 https://doi.org/10.1242/jeb.072751

680 Stockdale, W. T., Lemieux, M. E., Killen, A. C., Zhao, J., Hu, Z., Riepsaame, J., Hamilton, N., Kudoh, T.,
681 Riley, P. R., van Aerle, R., Yamamoto, Y., & Mommersteeg, M. T. M. (2018). Heart Regeneration in
682 the Mexican Cavefish. *Cell Reports*, *25*(8), 1997-2007.e7.
683 https://doi.org/10.1016/j.celrep.2018.10.072

684 Straka, H., Simmers, J., & Chagnaud, B. P. (2018). A New Perspective on Predictive Motor Signaling.
685 *Current Biology*, *28*(5), R232–R243. https://doi.org/10.1016/j.cub.2018.01.033

686 Tan, D., Patton, P., & Coombs, S. (2011). Do blind cavefish have behavioral specializations for active
687 flow-sensing? *Journal of Comparative Physiology A*, *197*(7), 743–754.

688 Teyke, T. (1985). Collision with and avoidance of obstacles by blind cave fish Anoptichthys jordani
689 (Characidae). *Journal of Comparative Physiology A*, *157*(6), 837–843.

690 Teyke, T. (1990). Morphological differences in neuromasts of the blind cave fish Astyanax hubbsi and
691 the sighted river fish Astyanax mexicanus. *Brain, Behavior and Evolution*, *35*(1), 23–30.

692 Trapani, J. G., & Nicolson, T. (2011). Mechanism of spontaneous activity in afferent neurons of the
693 zebrafish lateral-line organ. *The Journal of Neuroscience: The Official Journal of the Society for*
694 *Neuroscience*, *31*(5), 1614–1623. https://doi.org/10.1523/JNEUROSCI.3369-10.2011

695 Tricas, T. C., & Highstein, S. M. (1991). Action of the octavolateralis efferent system upon the lateral
696 line of free-swimming toadfish, Opsanus tau. *Journal of Comparative Physiology A*, *169*(1), 25–37.
697 https://doi.org/10.1007/BF00198170

698 Uysal, S. A., Erden, Z., Akbayrak, T., & Demirtürk, F. (2010). Comparison of balance and gait in
699 visually or hearing impaired children. *Perceptual and Motor Skills*, *111*(1), 71–80.

700 Van Trump, W. J., Coombs, S., Duncan, K., & McHenry, M. J. (2010). Gentamicin is ototoxic to all hair
701 cells in the fish lateral line system. *Hearing Research*, *261*(1–2), 42–50.

702 Varatharasan, N., Croll, R. P., & Franz-Odendaal, T. (2009). Taste bud development and patterning in
703 sighted and blind morphs of Astyanax mexicanus. *Developmental Dynamics: An Official Publication*
704 *of the American Association of Anatomists*, *238*(12), 3056–3064.
705 https://doi.org/10.1002/dvdy.22144

706 Von Campenhausen, C., Riess, I., & Weissert, R. (1981). Detection of stationary objects by the blind
707 cave fish Anoptichthys jordani (Characidae). *Journal of Comparative Physiology*, *143*(3), 369–374.

708 Warren, W. C., Boggs, T. E., Borowsky, R., Carlson, B. M., Ferrufino, E., Gross, J. B., Hillier, L., Hu, Z.,
709 Keene, A. C., & Kenzior, A. (2021). A chromosome-level genome of Astyanax mexicanus surface fish

for comparing population-specific genetic differences contributing to trait evolution. *Nature Communications*, *12*(1), 1–12.

Wickham, H. (2007). Reshaping Data with the **reshape** Package. *Journal of Statistical Software*, *21*(12). https://doi.org/10.18637/jss.v021.i12

Wickham, H. (2009). *The split-apply-combine strategy for data analysis*.

Wickham, H., François, R., Henry, L., & Müller, K. (2019). dplyr: A Grammar of Data Manipulation. R package version 0.8. 0.1. *Retrieved January*, *13*, 2020.

Wilke, C. O. (2019). cowplot: Streamlined plot theme and plot annotations for 'ggplot2.' *R Package Version 0.9*, *4*.

Windsor, S. P., Tan, D., & Montgomery, J. C. (2008). Swimming kinematics and hydrodynamic imaging in the blind Mexican cave fish (Astyanax fasciatus). *Journal of Experimental Biology*, *211*(18), 2950–2959.

Yamamoto, Y., Byerly, M. S., Jackman, W. R., & Jeffery, W. R. (2009). Pleiotropic functions of embryonic sonic hedgehog expression link jaw and taste bud amplification with eye loss during cavefish evolution. *Developmental Biology*, *330*(1), 200–211.

Yoffe, M., Patel, K., Palia, E., Kolawole, S., Streets, A., Haspel, G., & Soares, D. (2020). Morphological malleability of the lateral line allows for surface fish (Astyanax mexicanus) adaptation to cave environments. *Journal of Experimental Zoology Part B: Molecular and Developmental Evolution*, *334*(7–8), 511–517. https://doi.org/10.1002/jez.b.22953

Yoshizawa, M., Gorički, Š., Soares, D., & Jeffery, W. R. (2010). Evolution of a Behavioral Shift Mediated by Superficial Neuromasts Helps Cavefish Find Food in Darkness. *Current Biology*, *20*(18), 1631–1636. https://doi.org/10.1016/j.cub.2010.07.017

Yoshizawa, M., Jeffery, W. R., Netten, S. M. van, & McHenry, M. J. (2014). The sensitivity of lateral line receptors and their role in the behavior of Mexican blind cavefish (Astyanax mexicanus). *Journal of Experimental Biology*, *217*(6), 886–895. https://doi.org/10.1242/jeb.094599

Yoshizawa, M., Yamamoto, Y., O'Quin, K. E., & Jeffery, W. R. (2012). Evolution of an adaptive behavior and its sensory receptors promotes eye regression in blind cavefish. *BMC Biology*, *10*(1), 1–16.

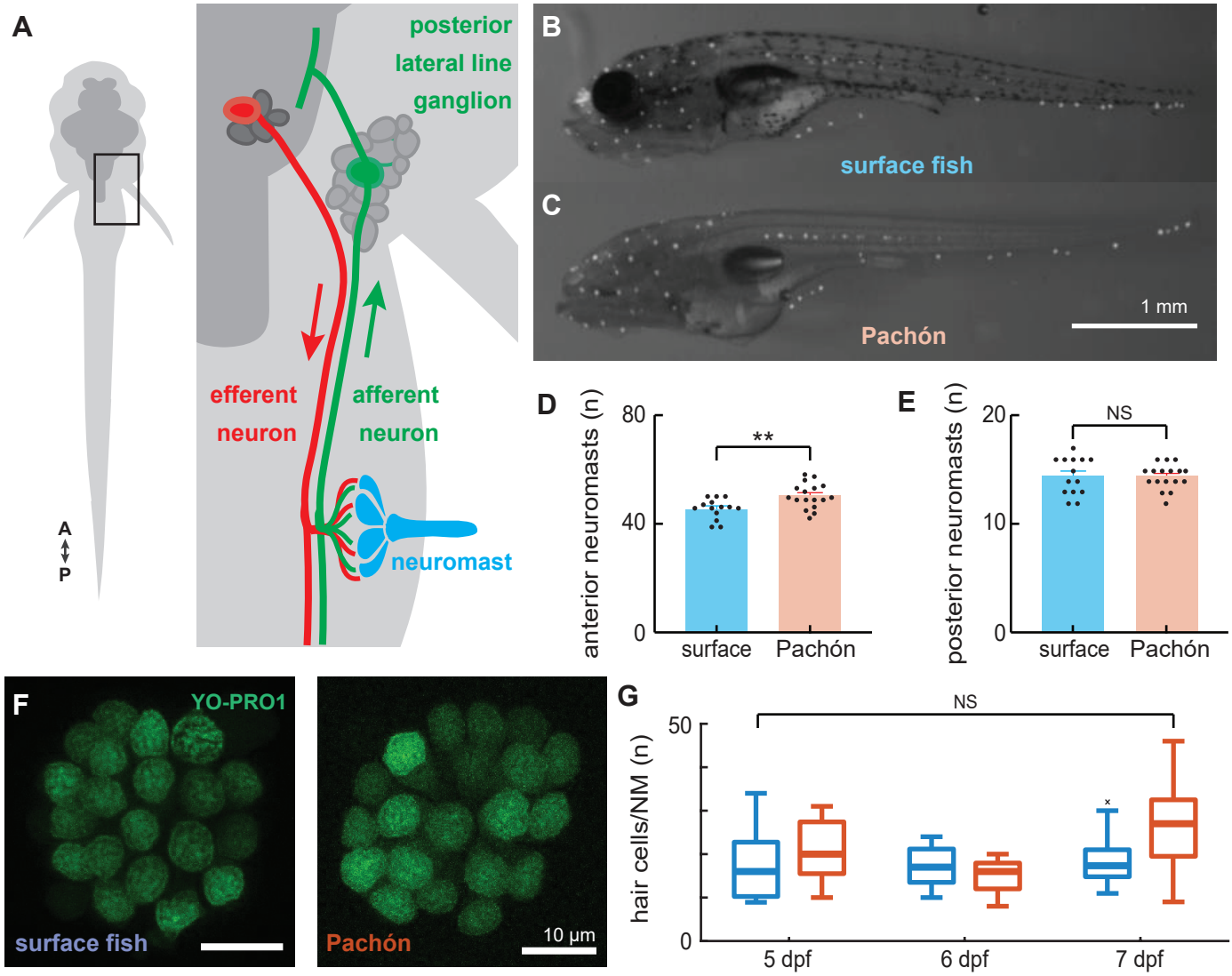
A
posterior
lateral line
ganglion
efferent
neuron
afferent
neuron
neuromast
A
P
B
surface fish
C
Pachón
1 mm
D
anterior neuromasts (n)
80
40
0
**
surface
Pachón
E
posterior neuromasts (n)
20
10
0
NS
surface
Pachón
F
YO-PRO1
surface fish
Pachón
10 µm
G
hair cells/NM (n)
50
0
NS
5 dpf
6 dpf
7 dpf

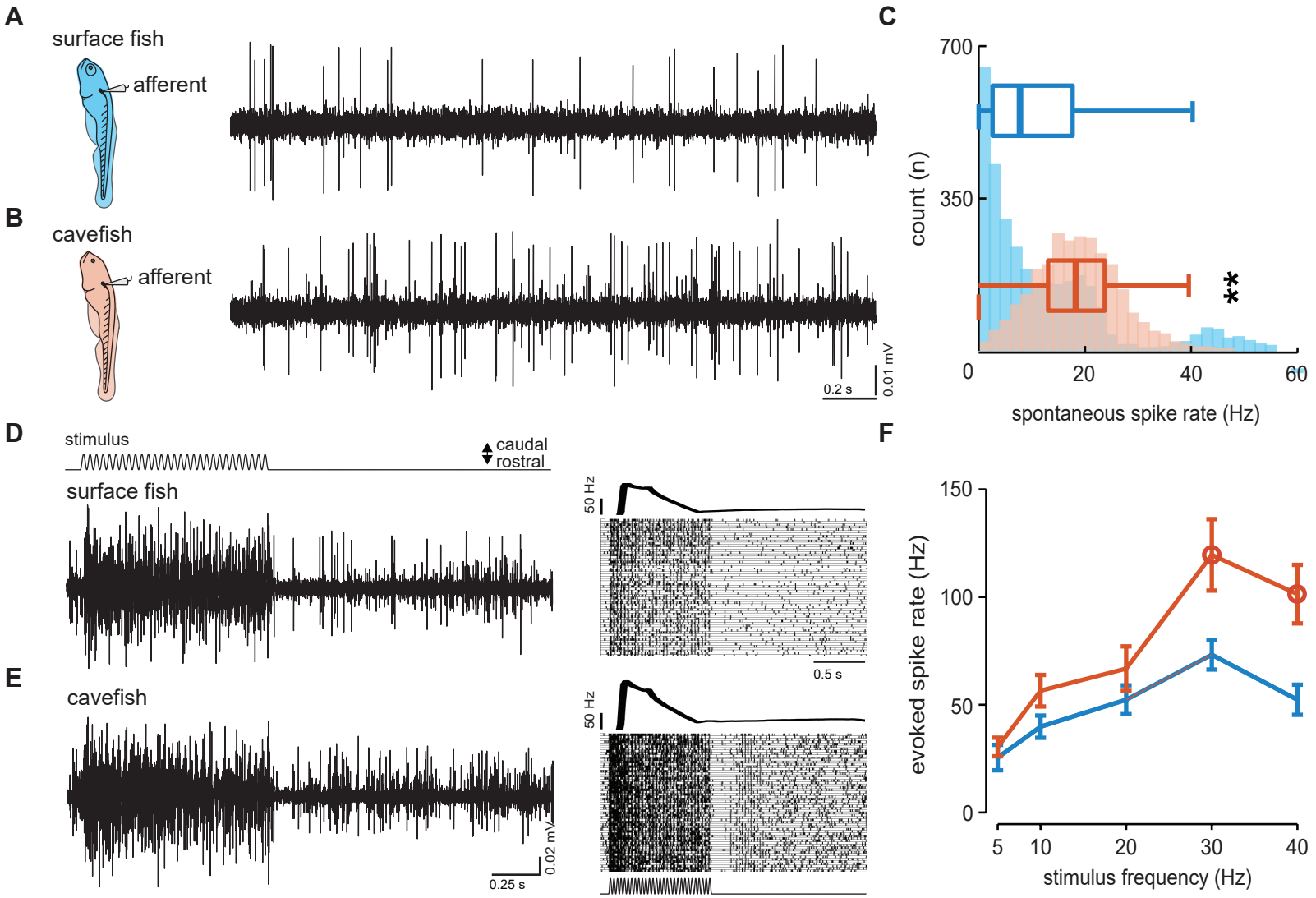
A
surface fish
afferent
B
cavefish
afferent
0.2 s
0.01 mV
C
700
350
0
count (n)
20
40
60
spontaneous spike rate (Hz)
**
D
stimulus
caudal
rostral
surface fish
50 Hz
0.5 s
E
cavefish
0.02 mV
0.25 s
50 Hz
F
150
100
50
0
evoked spike rate (Hz)
5
10
20
30
40
stimulus frequency (Hz)

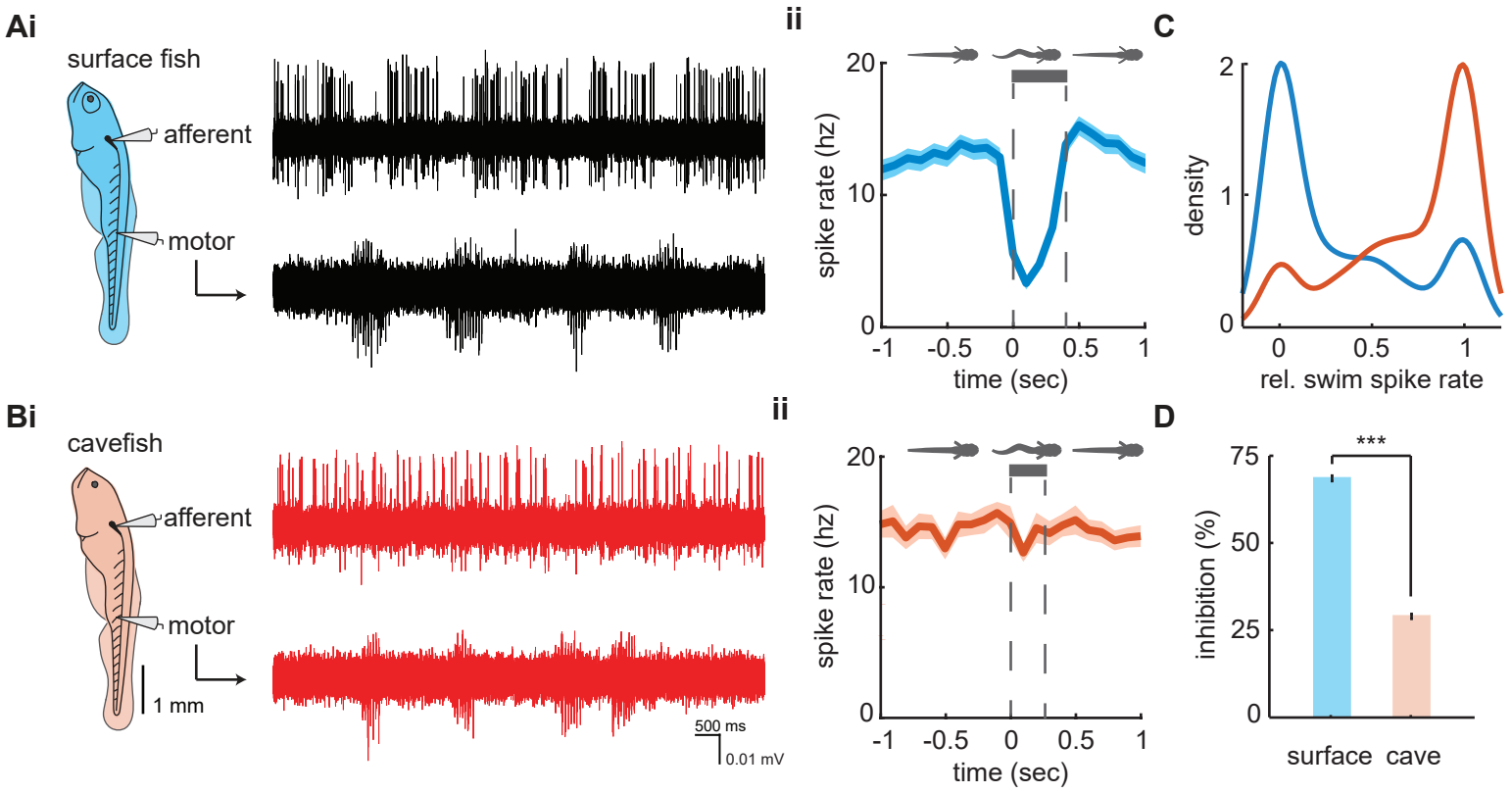
Ai
surface fish
afferent
motor
ii
spike rate (hz)
time (sec)
C
density
rel. swim spike rate
Bi
cavefish
afferent
motor
1 mm
500 ms
0.01 mV
ii
spike rate (hz)
time (sec)
D
inhibition (%)
***
surface
cave

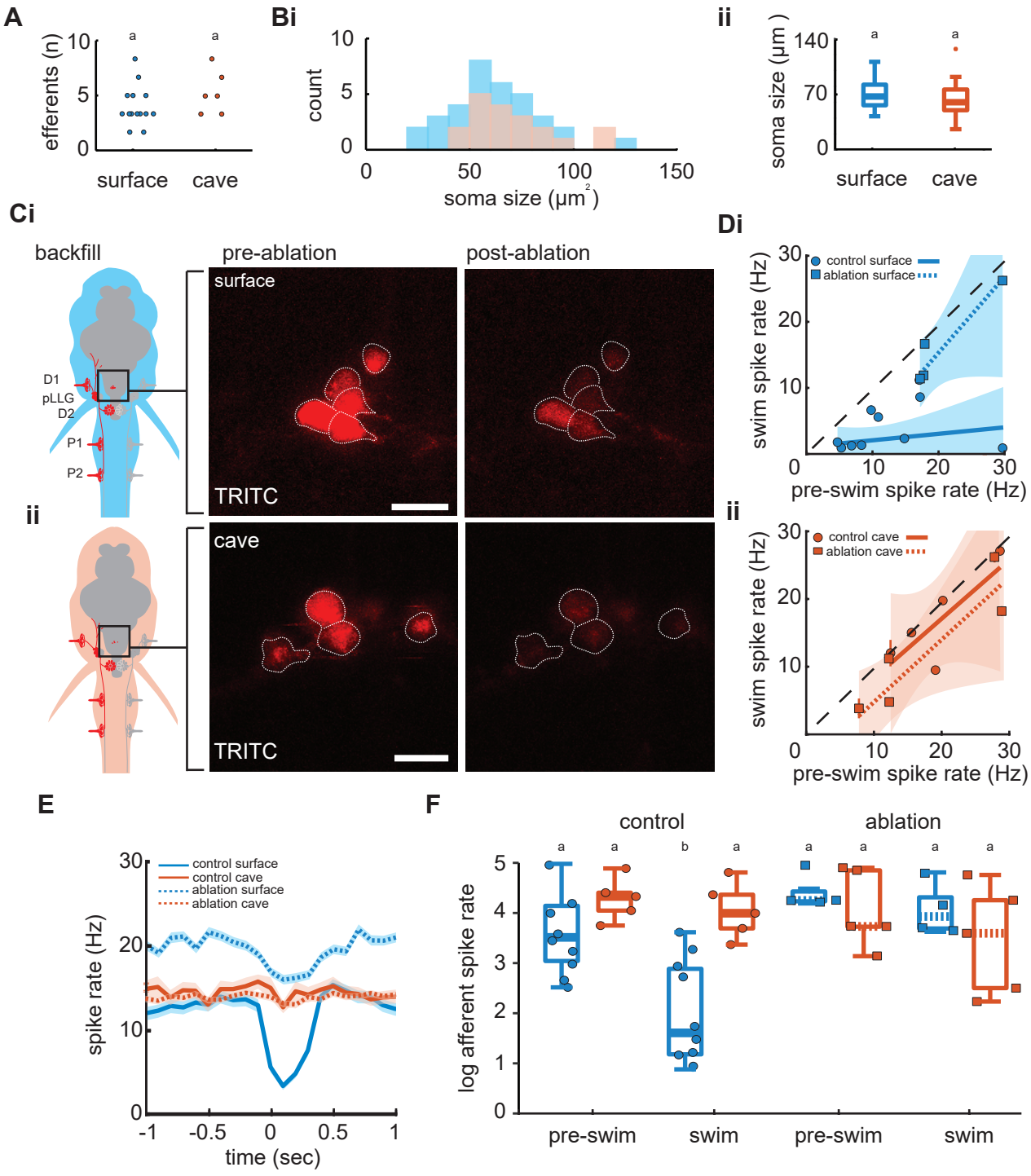
A
efferents (n)
10
5
0
a
a
surface
cave
Bi
count
10
5
0
0
50
100
150
soma size (μm²)
ii
soma size (μm)
140
70
0
a
a
surface
cave
Ci
backfill
pre-ablation
post-ablation
surface
TRITC
D1
pLLG
D2
P1
P2
ii
cave
TRITC
Di
control surface
ablation surface
swim spike rate (Hz)
pre-swim spike rate (Hz)
0
10
20
30
ii
control cave
ablation cave
swim spike rate (Hz)
pre-swim spike rate (Hz)
E
control surface
control cave
ablation surface
ablation cave
spike rate (Hz)
30
20
10
0
-1
-0.5
0
0.5
1
time (sec)
F
control
ablation
log afferent spike rate
5
4
3
2
1
0
a
a
b
a
a
a
a
a
pre-swim
swim
pre-swim
swim

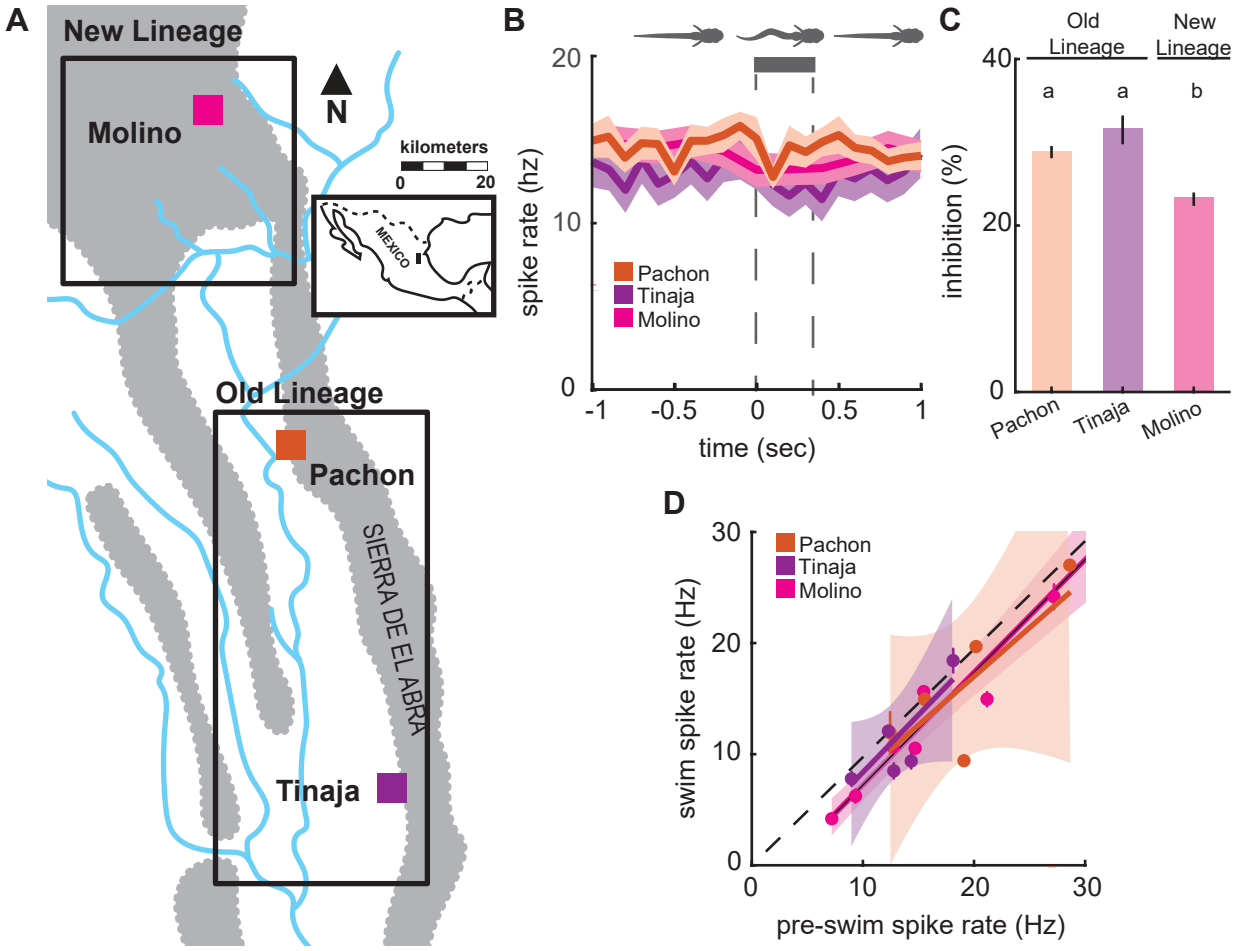
A
New Lineage
Molino
N
kilometers
0
20
MEXICO
Old Lineage
Pachon
SIERRA DE EL ABRA
Tinaja
B
spike rate (hz)
20
10
0
-1
-0.5
0
0.5
1
time (sec)
Pachon
Tinaja
Molino
C
Old Lineage
New Lineage
a
a
b
inhibition (%)
40
20
0
Pachon
Tinaja
Molino
D
swim spike rate (Hz)
30
20
10
0
0
10
20
30
pre-swim spike rate (Hz)
Pachon
Tinaja
Molino